Multiple-length-scale patterning of magnetic nanoparticles by stamp assisted deposition

2008 J. Phys.: Condens. Matter 20 204144

(http://iopscience.iop.org/0953-8984/20/20/204144)

IOP PUBLISHING JOURNAL OF PHYSICS: CONDENSED MATTER

J. Phys.: Condens. Matter **20** (2008) 204144 (5pp) doi:10.1088/0953-8984/20/20/204144

Multiple-length-scale patterning of magnetic nanoparticles by stamp assisted deposition

M Cavallini[1], E Bystrenova[1], M Timko[2], M Koneracka[2], V Zavisova[2] and P Kopcansky[2]

[1] CNR-ISMN, Via Gobetti 101, 40129 Bologna, Italy
[2] Institute of Experimental Physics, Slovak Academy of Sciences, Watsonova 47, 040 01 Košice, Slovakia

E-mail: Massimiliano.Cavallini@bo.ismn.cnr.it

Received 5 April 2008
Published 1 May 2008
Online at stacks.iop.org/JPhysCM/20/204144

Abstract

Control of the size and spatial distribution of materials at multiple length scales is one of the most compelling issues in nanotechnology research. We report a multiple-length-scale patterning of pure magnetic particles as well as biocompatible magnetic particles based on a printing technique named micro-injection molding in capillaries. The magnetic particles were prepared by a technique of co-precipitation of ferric and ferrous salts in an alkali medium. We demonstrate that the morphology and the size of the patterning nanoparticles can be controlled by simply controlling the concentration of the solution. Our method exploits the self-organization of the nanoparticles in a solution confined between a stamp and the surfaces of a substrate, exploiting confinement and competing interactions between the adsorbate and the substrate. Our approach represents a remarkable example of an integrated top-down/bottom-up process.

1. Introduction

Magnetic nanoparticles (MNPs) with appropriately tailored shells can have unique magnetic properties not present in other materials. Due to these peculiar properties, MNPs have been proposed as potential candidates for several versatile applications such as in high density magnetic storage [1], plasmon waveguides [2], one-dimensional nanostructure arrays [3], Coulomb blockade devices [4], nanowires [5] and more recently in spintronics [6]. For most of these applications the fabrication of thin films and/or artificially organized patterns [7] is certainly a crucial issue. Furthermore several possibilities are offered by nanotechnological applications; in particular, breakthroughs are expected in the patterning of biologically active substances [8] coupled to magnetic particles.

A major effort in nanotechnology has been devoted to the patterning of active materials into size and shape controlled structures, because of the ambitious goal of controlling physical properties through the control of materials' length scales [9]. For this purpose earlier work has reported the use of microcontact printing [10] combined with layer-by-layer self-assembly [11], and applying electron beam treatment to the formed layers of nanoparticles [12] as well as focused ion beams [13] was reported. Here we propose the application of a soft lithographic method named micro-injection molding in capillaries [14] to obtain a pattern of sub-micrometric stripes and dots of the Fe_3O_4 nanoparticles.

2. Experimental methods and results

2.1. Preparation and characterization of magnetic fluid

The synthesis of our aqueous magnetic fluid was based on co-precipitation of Fe(II) and Fe(III) salts with $NaOH_4$ at 60 °C. In a typical synthesis to obtain 1 g of Fe_3O_4 precipitate, 0.86 g of $FeCl_2{\cdot}4H_2O$ and 2.35 g of $FeCl_3{\cdot}6H_2O$ were dissolved in 40 ml deionized water with vigorous stirring, such that $Fe^{3+}/Fe^{2+} = 2$. As the solution was heated to 80 °C a solution of 100 mg of neat lauric acid in 5 ml acetone was added, followed by 5.6 ml of 25% NH_4OH. After that 1 g more lauric acid was added to the suspension. The crystal growth was allowed to

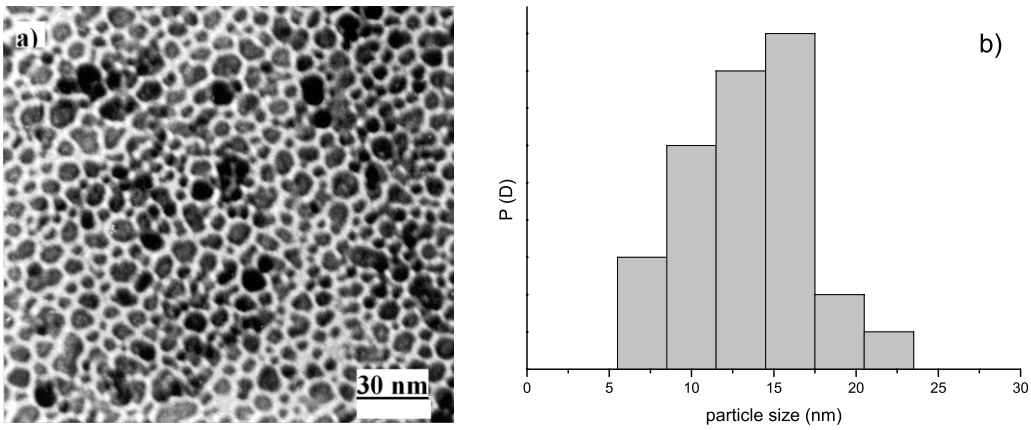

Figure 1. (a) TEM image of magnetic particles stabilized by lauric acid. (b) Size distribution of Fe_3O_4 nanoparticles.

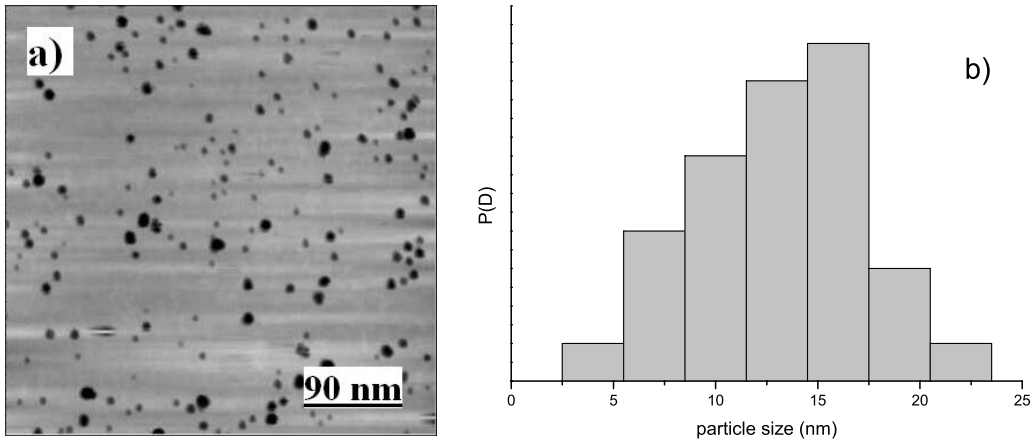

Figure 2. (a) AFM image of magnetic particles stabilized by lauric acid cast on a mica surface. (b) Size distribution of Fe_3O_4 nanoparticles.

proceed for 30 min at 80 °C with constant stirring to produce a stable water based suspension, which was then cooled slowly to room temperature. The suspension was precipitated with H_2SO_4. The precipitates were isolated from the solvent by magnetic decantation. The washing–decantation method was applied several times for the removal of excess lauric acid. Its effective removal was confirmed by the lack of lauric acid in the magnetic decantation supernatant.

Magnetic properties of Fe_3O_4 nanoparticles were estimated using a SQUID magnetometer while the size (diameter (d)) and distribution (standard deviation (σ)) were measured both from transmission electron microscopy (TEM) and atomic force microscopy (AFM). Examination by TEM was done using a Tesla BS 500 microscope normally operated at 90 kV and 80 000× magnification by a replication technique. A drop of Fe_3O_4 nanoparticle suspension containing 5×10^{14} # particles of cm^{-3} was deposited on the 400 mesh copper grid and air dried before the picture was taken. A TEM image of spherical magnetic particles stabilized by lauric acid and the histogram of the size distribution are shown in figure 1.

Figure 1 indicates that lauric acid provides an effective stabilization for dispersing Fe_3O_4 nanoparticles in an aqueous medium. About 450 particles were analyzed in the TEM image data [15]. The mean diameter and σ measured from the TEM images were $d = 12.9$ nm and $\sigma = 0.22$, respectively.

AFM characterization of Fe_3O_4 nanoparticles was done using a Nanoscope IIIa Multimode SPM (Digital Instruments, Santa Barbara, CA) and its image analysis software, as well as with our own. The particles were imaged in tapping mode at a scan rate between 1 and 3 Hz using rectangular silicon (Si) cantilevers/probes (Nanosensors, Wetzlar–Blankenfeld, Germany). AFM characterization of patterned samples was done using a commercial AFM SMENA (NT-MDT) in semi-contact mode in air. Silicon NT-MDT cantilevers, NSG10 series, were used in our experiments. All images are unfiltered. The topographic images were corrected line by line for background trend effects by removal of the second-order polynomial fitting. Image analysis was carried out *ex situ* with image analysis software IMAGE-SXM 1.84 and analyses of the line profiles of autocorrelation spectra were carried out with Igor Pro 4.0. Figure 2 shows an AFM image of Fe_3O_4 nanoparticles and the corresponding histogram of the size distribution.

The mean diameter and σ measured from AFM images were $d = 12.1$ nm and 0.21, respectively, which are in good agreement with the TEM measurements. Magnetic properties of Fe_3O_4 nanoparticles coated with lauric acid as a surfactant were characterized using a SQUID magnetometer at room temperature. As expected they exhibit superparamagnetic behavior without coercivity. The saturation magnetization

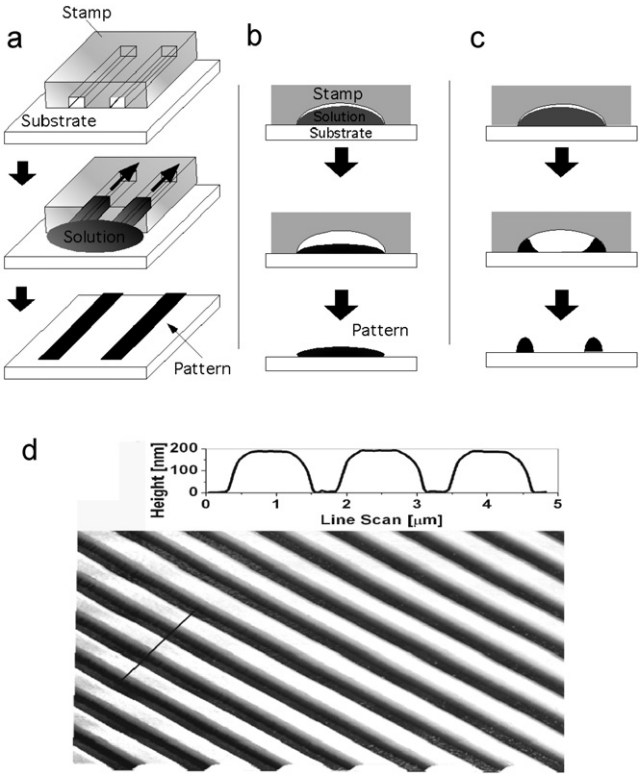

Figure 3. (a) General scheme of micro-injection molding in capillaries (MIMIC). (b) Detail of the last step of evaporation in the concentrated regime and (c) in the diluted regime. (d) AFM image of the PDMS stamp used in this work with the line profile.

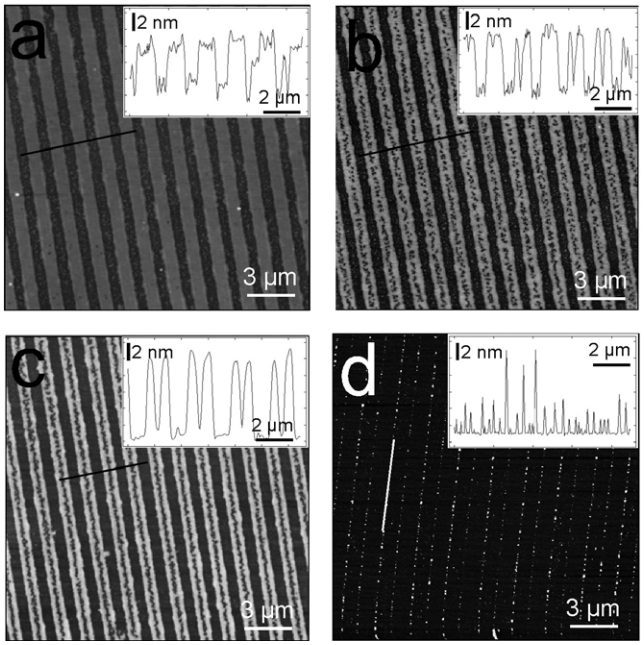

Figure 4. Evolution of the morphology corresponding to a variation of the solution volume inside the μ-channels: (a) full ($\sim$100%) μ-channels; (b) $\sim$75% of the volume; (c) $\sim$50% of the volume; (d) $\sim$25% of the volume.

using a concentration of 120 mg ml^{-1} was estimated to be 10.2 mT.

2.2. *Patterning of Fe_3O_4 nanoparticles*

Micro-injection molding in capillaries (MIMIC) is a well known unconventional lithographic method [16, 17] used to pattern several functional materials, such as organic and inorganic semiconductors [18], biological molecules [19] and other materials [20, 21]. Here MIMIC has been used to fabricate sub-micrometric stripes of Fe_3O_4 nanoparticles; its scheme is shown in figure 3(a).

In MIMIC a stamp made of polydimethylsiloxane (PDMS; Sylgard 184 Down Corning), whose motif consists of parallel grooves, is placed in contact with the surface. PDMS stamps were prepared by replica molding of a structured master. The curing process was carried for 6 h at 60 °C. Once cured, the replica is peeled off from the master and washed in pure ethanol.

In our experiments the PDMS stamp motif consists of parallel lines with a periodicity of 1.4 μm, width at half-height 500 and 200 nm. An AFM image of the stamp is shown in the figure 3(d). The grooves between the protrusions in contact with the surface form the microcavities, which once in contact with the substrate delimit the sub-micrometric channels (μ-channels) 800 nm in width (10% of the width contraction is due to the stamp deformation) and 200 nm high. When the solution is deposited at the open end of the stamp, the liquid spontaneously fills the μ-channels under the effect of capillary forces. After the complete evaporation of the solvent (24 h at room temperature) the stamp is gently removed and the samples investigated by AFM. The self-organization of the solute enters into play at the later stages of shrinking, when the solution reaches supersaturation. Depending on the nature of the solvent the evaporation, which can occur through the stamp or only from the open part of the channels, different kinds of patterns can be obtained. Using water, or polar solvent, the solvent evaporation occurs from the open part of the channels, inducing a small flux of material that occasionally compromises the homogeneity of the pattern. Spatially organized nanodots or continuous μ-stripes are fabricated, exploiting self-organization and dewetting [22] of Fe_3O_4 nanoparticles. Depending on the concentration of the solution, several kinds of patterns can be obtained by MIMIC. If the solution reaches supersaturation when the μ-channel is still full of solution (high concentrate regime), the pattern replicates the size of the μ-channel (see figure 3(a)). On the other hand if the solution reaches supersaturation when the major part of the solvent is evaporated and the volume of the residual solution is not enough to completely fill the μ-channel, the solution tends to accumulate on the boundaries of the μ-channel giving rise to some defects in the μ-stripes (see figure 3(b)) or split lines as shown in figure 3(c) (diluted regime).

For our experiment we have used Fe_3O_4 nanoparticles functionalized by lauric acid as described in section 2.1; however similar results were obtained with nanoparticles functionalized by other surfactants. Freshly cleaved mica was used as a prototype surface for this experiment. Figure 4 shows the evolution of the morphology of Fe_3O_4 sub-micrometric

stripes obtained by using 10 mg l^{-1} of Fe_3O_4 nanoparticles dissolved in water. The images of the morphology were acquired by AFM at different parts of the samples. Due to high viscosity of the Fe_3O_4 nanoparticles solution it does not completely fill the μ-channels before solvent evaporation; this induces a gradient in the volume of the solution inside the channel. This gives rise to a different kind of pattern, depending on the position inside the μ-channels. The effective volume in each part was estimated from the volume of the deposited material. Equivalent results can be obtained simply using more diluted and less viscous solution to enable complete filling of the μ-channels. When the solution completely fills the μ-channel, the resulting pattern consists of homogeneous lines (figure 4(a)) whose average height is approximately 9.0 $\pm$ 1.1 nm, with 1.4 μm periodicity that perfectly reproduces the periodicity of the stamp. The thickness of the μ-stripes corresponds to the formation of a single monolayer of Fe_3O_4 nanoparticles. Occasionally some defects consisting of holes and dots are present on the stripes. These defects are 8.9 $\pm$ 1.1 nm thick and less than 20 nm in width. The exact width cannot measured due to tip deconvolution, but this strongly suggests that these defects are formed by the absence of a single cluster. The number of the defects increases dramatically when moving in the zones where the volume of the solution inside the μ-channel is reduced. In this case the nanoparticle density is not enough to form a complete monolayer. Figure 4(b) thus shows the case where about 75% of the volume is filled by the solution. Here the defects exhibit the same thickness behavior as a monolayer. However, further reducing the volume of the solution to less than 50% of the total volume of the μ-channels results in splitting of the lines of nanoparticles, as seen in figure 4(c). This is expected in the diluted regime, as schematized in figure 3(c).

As the quantity of deposited material decreases further below a certain threshold, corresponding to a very diluted regime, where the estimated value of deposited material is $\sim$30 ng cm^{-2}, the morphology of the patterns changes dramatically. This is shown in figure 4(d) where droplets, instead continuous stripes, are formed. As seen from the line profile measured along the printed lines, the droplets exhibit different heights, which correspond to the formation of aggregates of a few nanoclusters. Figure 5 shows the statistical analysis of the nanocluster distribution in a very diluted regime; in particular figure 5(a) shows the 2D height–height correlation function ($g(r)$) of figure 4(a). As expected, the line profile of $g(r)$ measured perpendicular to the μ-stripes shows a well defined periodicity. This periodicity is imposed by the stamp; however, as shown in figure 5(c), the line profile of $g(r)$ measured parallel to the printed lines also shows the spatial correlation among the nanoclusters, which is seen to extend up to the eighth neighbor.

2.3. Summary

In conclusion, we have applied the micro-injection molding in capillaries method directly to magnetic nanoparticles to yield a patterned thin film with submicron periodic features, and a vertical resolution of a monolayer. The pitch reported in our work is essentially due to the stamp used. The resolution limit of the method has not been fully explored, but we are confident that at the moment just the dimension of the stamp used limits us. Our procedure is a single-step process, versatile and reproducible, allowing for transfer of motifs at sub-micrometer scale. Here, we used Fe_3O_4 nanoparticles as this is a common material, but we can in principle easily extend this process to many other soluble nanoparticles. Our approach extends the perspectives to soft lithography applied to magnetic nanoparticles. New developments are in progress and include the confinement growth inside a two-dimensional cell with different shapes: by reducing the size of the confinement and by applying magnetic fields during the deposition, one gets interesting self-organizing properties of the magnetic nanoparticles [23–25]. Furthermore, in order to fabricate functional devices, MIMIC could lead to the integration of nanoparticles with other functional materials such as organic semiconductors [26], biological molecules [8], and a possible combination with electrochemical systems [27].

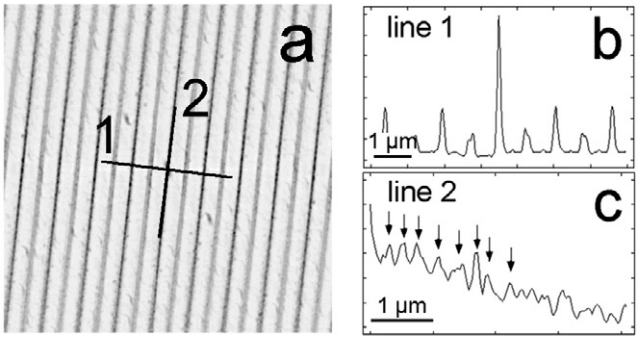

Figure 5. (a) 2D height–height correlation function $g(r)$ of Fe_3O_4 nanoparticles of figure 4(c). (b) Line profile of $g(r)$ measured parallel (line 1) and (c) perpendicular (line 2) to the printed μ-stripes. The peaks in the correlation function are indicated with black arrows.

Acknowledgments

This work was supported by the ESF-EURYI project DYMOT, EU-ESF FUNSMART2, and VEGA 6166 and the Slovak Research and Development Agency under the contracts APVV-26-026505, APVV-0173-06 and 51-027904. EB is supported by EU-Project BIODOT (NMP4-CT-2006-032652).

References

[1] Sato H and Takayuki H 2007 *J. Nanosci. Nanotechnol.* **7** 225
[2] Maier S A *et al* 2003 *Nat. Mater.* **2** 229
[3] Cheng J Y, Zhang F, Chuang V P, Mayes A M and Ross C A 2006 *Nano Lett.* **6** 2099
[4] Chen W, Ahmed H and Nakazoto K 1995 *Appl. Phys. Lett.* **66** 3383
[5] Zhang D H, Liu Z Q, Han S, Li C, Lei B, Stewart M P, Tour J M and Zhou C W 2004 *Nano Lett.* **4** 2151
[6] Podar P, Woods G T, Srinath S and Srikanth H 2005 *IEEE Trans. Nanotechnol.* **4** 59

[7] Cavallini M, Gomez-Segura J, Ruiz-Molina D, Massi M, Albonetti C, Rovira C, Veciana J and Biscarini F 2005 *Angew. Chem. Int. Edn* **44** 888
[8] Bystrenova E, Facchini M, Cavallini M, Cacace M G and Biscarini F 2006 *Angew. Chem. Int. Edn* **45** 4779
[9] Cavallini M, Stoliar P, Moulin J F, Surin M, Leclere P, Lazzaroni R, Breiby D W, Andreasen J W, Nielsen M M, Sonar P, Grimsdale A C, Müllen K and Biscarini F 2005 *Nano Lett.* **5** 2422–5
[10] Palacin S, Hidber P C, Bourgoin J-P, Miramond C, Fermon C and Whitesides G M 1996 *Chem. Mater.* **8** 1316
[11] Xue W, Cui T H, Lei X J, Li D B, Shao R and Bonnell D A 2005 *J. Mater. Res.* **20** 712
[12] Erokhina S, Berzina T, Cristofolini L, Shchukin D, Sukhorukov G, Musa L, Erokhin V and Fontana M P 2004 *J. Magn. Magn. Mater.* **272** 1353
[13] Anders S, Sun S, Murray C B, Rettner C T, Best M E, Thomson T, Albrecht M, Thiele J U, Fullerton E E and Terris B D 2002 *Microelectron. Eng.* **61** 569
[14] Kim E, Xia Y and Whitesides G M 1995 *Nature* **376** 581
[15] Popplewell J and Sakhnini L 1995 *J. Magn. Magn. Mater.* **149** 72
[16] Xia Y and Whitesides G M 1998 *Angew. Chem. Int.* **37** 550
[17] Cavallini M and Biscarini F 2003 *Nano Lett.* **3** 1269–71
[18] Cavallini M, Murgia M and Biscarini F 2001 *Nano Lett.* **1** 193–5
[19] Cavallini M, Aloisi G, Bracali M and Guidelli R 1998 *J. Electroanal. Chem.* **444** 75–81
[20] Cavallini M, Facchini M, Albonetti C and Biscarini F 2008 *Phys. Chem. Chem. Phys.* **10** 784
[21] Greco P, Cavallini M, Stoliar P, Quiroga S D, Dutta S, Zacchini S, Lapalucci M C, Morandi V, Milita S, Merli P G and Biscarini F 2008 *J. Am. Chem. Soc.* **130** 1177
[22] Cavallini M, Biscarini F, Gomez-Segura J, Ruiz D and Veciana J 2003 *Nano Lett.* **3** 1527
[23] Leoa G, Chushkin Y, Luby S, Majkova E, Kostic I, Ulmeanud M, Luchese A, Giersigf M and Hilgendorff M 2003 *Mater. Sci. Eng.* C **23** 949952
[24] Chushkin Y, Chitu L, Halahovets Y, Luby S, Majkova E, Satka A, Leo G, Giersig M, Hilgendorff M, Holy V and Konovalov O 2006 *Mater. Sci. Eng.* C **26** 1136–40
[25] Chitu L, Chushkin Y, Luby S, Majkova E, Satka A, Ivan J, Smrcok L, Buchal A, Giersig M and Hilgendorff M 2007 *Mater. Sci. Eng.* C **27** 2328
[26] Menozzi C, Corradini V, Cavallini M, Biscarini F, Betti M and Mariani C 2003 *Thin Solid Films* **428** 227
[27] Innocenti M, Cattarin S, Cavallini M, Loglio F and Foresti M L 2002 *J. Electroanal. Chem.* **532** 219